Clinical Neuroradiology
https://doi.org/10.1007/s00062-023-01325-8

ORIGINAL ARTICLE

Clinical Efficiency of an Artificial Intelligence-Based 3D-Angiography for Visualization of Cerebral Aneurysm: Comparison with the Conventional Method

Kojiro Ishikawa[1] · Takashi Izumi[1] · Masahiro Nishihori[1] · Takahiro Imaizumi[2] · Shunsaku Goto[1] · Keita Suzuki[1] · Kinya Yokoyama[1] · Fumiaki Kanamori[1] · Kenji Uda[1] · Yoshio Araki[1] · Ryuta Saito[1]

Received: 10 April 2023 / Accepted: 31 May 2023

Abstract

Purpose Artificial intelligence (AI)-based three-dimensional angiography (3D-A) was reported to demonstrate visualization of cerebral vasculature equivalent to that of three-dimensional digital subtraction angiography (3D-DSA). However, the applicability and efficacy of the AI-based 3D-A algorithm have not yet been investigated for 3D-DSA micro imaging. In this study, we evaluated the usefulness of the AI-based 3D-A in 3D-DSA micro imaging.

Materials and Methods The 3D-DSA micro datasets of 20 consecutive patients with cerebral aneurysm (CA) were reconstructed with 3D-DSA and 3D-A. Three reviewers compared 3D-DSA and 3D-A in terms of qualitative parameters (degrees of visualization of CA and the anterior choroidal artery [AChA]) and quantitative parameters (aneurysm diameter, neck diameter, parent vessel diameter, and visible length of AChA).

Results Qualitative evaluation of diagnostic potential revealed that visualization of CA and the proximal to middle parts of the AChA with 3D-A was equal to that with conventional 3D-DSA; in contrast, visualization of the distal part of the AChA was lower with 3D-A than with 3D-DSA. Further, regarding quantitative evaluation, the aneurysm diameter, neck diameter, and parent vessel diameter were comparable between 3D-A and 3D-DSA; in contrast, the visible length of the AChA was lower with 3D-A than with 3D-DSA.

Conclusions The AI-based 3D-A technique is feasible and evaluable visualization of cerebral vasculature with respect to quantitative and qualitative parameters in 3D-DSA micro imaging. However, the 3D-A technique offers lower visualization of such as the distal portion of the AChA than 3D-DSA.

Keywords Artificial Intelligence · Deep learning · Cerebral aneurysm · Three-dimensional digital subtraction angiography · Anterior choroidal artery

Abbreviations

2D-DSA Two-dimensional digital subtraction angiography
3D-A Three-dimensional angiography
3D-DSA Three-dimensional digital subtraction angiography
AChA Anterior choroidal artery
AI Artificial intelligence
AVM Arteriovenous malformation
CA Cerebral aneurysm
dAVF Dural arteriovenous fistula
ICA Internal carotid artery
VRT Volume rendering techniqu
WA Working angle

Code Availability syngo Dyna4D (X-Workplace VD20, Siemens Healthcare, GmbH, Forchheim Germany)

✉ Takashi Izumi
my-yuzu@med.nagoya-u.ac.jp

[1] Department of Neurosurgery, Nagoya University Graduate School of Medicine, Nagoya University, Nagoya, Japan

[2] Department of Advanced Medicine, Nagoya University Hospital, Nagoya, Japan

Introduction

The current criterion standard for the visualization of cerebral vasculature is two-dimensional digital subtraction angiography (2D-DSA) and three-dimensional digital subtraction angiography (3D-DSA) [1, 2]. With 3D-DSA, blood vessels can be visualized at any angle, allowing for a bet-

Published online: 03 July 2023

ter understanding of pathologies and spatial relationships between adjacent vascular structures. In the treatment of cerebral aneurysms (CAs), three-dimensional (3D) images of cerebral vasculature are essential for the identification of a sufficient working angle (WA) to plan endovascular treatment and to ensure efficacy and patient safety [3–6]. To obtain 3D-DSA images, most angiography systems require two rotational imaging runs: one without contrast (mask run) and the other with contrast (fill run). Furthermore, 3D-DSA separates vascular and nonvascular structures by subtracting the mask run from the fill run.

Recent studies described a novel method based on a single contrast-enhanced fill run image and artificial intelligence (AI) that shows digital subtraction angiography (DSA)-like 3D volumes of the cerebral vasculature [7–9]. In 2018, Montoya et al. demonstrated the technical feasibility of the new method [7]. In addition, Lang et al. reported the clinical feasibility of a similar AI-based algorithmic approach that allows for the acquisition of 3D angiographic datasets with no need for native mask runs, and the results were promising [8]. Moreover, they showed that AI-based 3D angiography (3D-A) was equivalent to 3D-DSA in the detailed analysis of the visualization of CA, dural arteriovenous fistula (dAVF), and arteriovenous malformation (AVM) [9].

The above-mentioned approaches are promising and can be used in clinical settings. However, the applicability and efficacy of the AI-based 3D-A algorithm have not yet been investigated for 3D-DSA micro (Siemens) imaging which has detailed vascular visualization performance. In this study, we evaluated the usefulness of the novel method in 3D-DSA micro imaging to facilitate the use of the prototype AI-based 3D-A technique in clinical practice.

Materials and Methods

Patients

This study was approved by the Bioethics Review Committee of our hospital, and informed consent was obtained from all the enrolled patients. All procedures performed in studies involving human participants were in accordance with the 1964 Helsinki declaration and its later amendments or comparable ethical standards. We retrospectively collected the data of 20 consecutive patients who underwent scheduled treatment for CA at our hospital from April 2021 to December 2021. The inclusion criteria regarding CA were as follows: no rupture, anterior circulation, maximum CA diameter of ≤ 10 mm, and no previous treatment for CA. Clinical data were collected by reviewing patient characteristics and clinical findings.

3D-A

The prototype 3D-A technique is a new post-processing technique for generating DSA-like 3D volumes with diagnostic image quality. While 3D-DSA requires two rotations, the AI-based 3D-A requires a single contrast-enhanced run to distinguish between vessels and adjacent structures. The core of the prototype 3D-A technique is an AI-based classification of contrast-enhanced vasculature, nonvascular anatomical background, and implants or devices using a deep learning-based approach (i.e., convolutional neural networks) [10]. The 3D-A algorithm requires training to learn the separation of contrasted vasculature from surrounding anatomical structures and materials (e.g., fat, bone, and metal implants) based on contrast-enhanced and subtracted datasets. The training process involved 98 3D-DSA datasets that were collected retrospectively in a random fashion to cover a variety of conditions. The algorithm from the training process was reported and validated in previous studies [8, 9], and in this study, we used a prototype software similar to the algorithm.

Image Acquisition

Cerebral angiography (including 2D-DSA and 3D-DSA micro) was performed using a biplane flat panel detector angiographic system (Artis Q biplane, Siemens Healthcare GmbH, Forchheim, Germany). All angiograms were performed under local anesthesia and intravenous conscious sedation using standard angiographic methods. A diagnostic or guiding catheter was positioned in the proximal internal carotid artery (ICA), and standard anterior-posterior and lateral projections were performed (2D-DSA). Next, rotational scans for all the patients were acquired using the standard acquisition protocol (5-second 3D-DSA micro) provided by the manufacturer. An initial rotational scan (native mask run) was followed by a second rotational scan (contrast-enhanced fill run), and each scan had a duration of 5 s. Following existing 3D-DSA micro protocols, each run yielded a total of 133 projected images at a rotation angle of 200°, with a detector dose of 0.36 µGy per projected image (voltage: 70 kV, detector element: 1024 × 1024, pixel count: 1 × 1 binning, projection size: 16 cm × 16 cm, increment: 1.5°/frame, frame rate: 30 frames/second).

Image Reconstruction

All image data (including mask run and fill run) were transferred to *syngo* X-Workplace (VD20B; Siemens Healthcare GmbH, Forchheim, Germany), a clinical and dedicated research workstation that runs the prototype software. 3D-DSA and 3D-A reconstructions were performed using the fill and native runs for 3D-DSA and only the fill run for

3D-A from the same 3D-DSA micro datasets. Thereafter, the angle suitable for treatment (WA), at which the neck of the aneurysm and the branching vessels can be well observed, was set by the surgeon using the 3D image, and the 2D-DSA image was taken after adjusting the C-arm.

For standardization, both 3D-DSA and 3D-A reconstructions used the same reconstruction parameters as conventional 3D-DSA protocol (kernel type: edge enhanced, image characteristics: smooth, mode of reconstruction: subtracted, image matrix: 512 × 512). In addition, the threshold in 3D-A for controlling the tolerance of the vasculature classification was set at 40% in all cases. To compare the appropriate 3D-DSA and 3D-A images, the diameter of the petrous portion of the ICA on the 2D-DSA image at the WA was measured, and each window level was adjusted to match the diameter of the petrous portion of the ICA on the volume rendering technique (VRT) image of the 3D-DSA and 3D-A images at the WA (Fig. 1).

Image Evaluation

After anonymization, 3D-DSA and 3D-A reconstruction data were pooled and randomized. Three experienced physicians (an interventional neuroradiologist with 10 years of clinical experience and two neurosurgeons with eight and nine years of clinical experience) were blinded to the type of reconstruction (based on the conventional subtraction method or the AI algorithm). The reviewers were not informed of the protocol for the two types of reconstructed images. Furthermore, the images were switched from page to page (but not side-by-side) such that they could be compared at any time. They compared 3D-DSA and 3D-A acquisitions in terms of the degree of delineation and visualization of the CA and the anterior choroidal artery (AChA), a branch of the ICA that is universal to all patients, for qualitative and quantitative parameters on a research workstation.

Fig. 1 The WA (working angle), which is the appropriate angle for treatment, was set using 3D-DSA (three-dimensional digital subtraction angiography), and 2D-DSA (two-dimensional digital subtraction angiography) was performed at the WA. To compare the appropriate 3D-DSA and 3D-A (three-dimensional angiography) images, the diameter of the petrous part of the vessel on the 2D-DSA image at WA was measured, and each window level was adjusted to match the diameter of the petrous part of the vessel on the VRT (volume rendering technique) image of the 3D-DSA and 3D-A images at WA

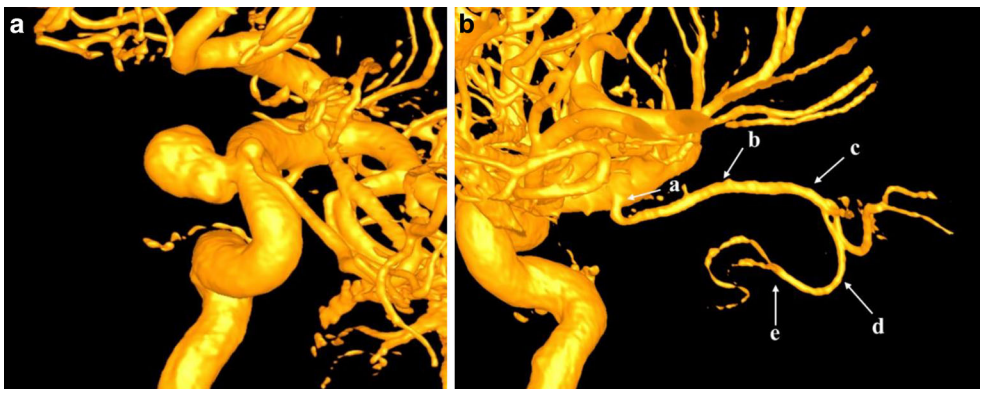

Fig. 2 An image of an aneurysm of the left ICA (internal carotid artery) for the evaluation of qualitative parameters is shown above. **a** The aneurysm evaluated at the WA (working angle). **b** The AChA (anterior choroidal artery) evaluated at an angle where it appeared longer. The figure shows five points (*a*, *b*, *c*, *d*, and *e*, in order from the origin of the AChA), which divide 4 cm of the vessel from its origin to form four equal sections

Evaluation of Qualitative Parameters

The visualization quality of the acquired 3D-DSA and 3D-A images for two items with the CA and the AChA was assessed in a consensus reading using a five-point system with the following grades: 4 = excellent (very high contrast, no artifacts), 3 = good (high contrast, minimal artifacts), 2 = compromised (reduced homogeneity of contrast and/or noticeable movement artifacts), 1 = heavily compromised (low contrast and/or strong movement artifacts), and 0 = not diagnostic (vasculature is not differentiable due to missing contrast and/or heavy artifacts). The two items were evaluated on a single image at each angle of the VRT image. The aneurysm was evaluated on the WA image, and the AChA was evaluated at five points (a, b, c, d, and e, which divide 4 cm of the vessel from its origin to form four equal sections) on the image such that the AChA appeared longer (Fig. 2a, b).

Evaluation of Quantitative Parameters

The degrees of accuracy of 3D-DSA and 3D-A images were evaluated using the VRT images. As in the qualitative evaluation and using a single image, CA was evaluated at the WA, and the AChA was evaluated at an angle such that it appeared longer. The aneurysm diameter at a designated location, the neck diameter, and the parent vessel diameter 5 mm distal and proximal to the neck were measured by the reviewers using the standard tools of the prototype workstation (Fig. 3a). In addition, the reviewers measured the length of the AChA to a defined arbitrary point (d1) and the length that they could not recognize as a vessel (d2). These lengths (d1 and d2) were used to calculate the percentage of vessel length that could be visualized (d1 – d2/d1) (Fig. 3b).

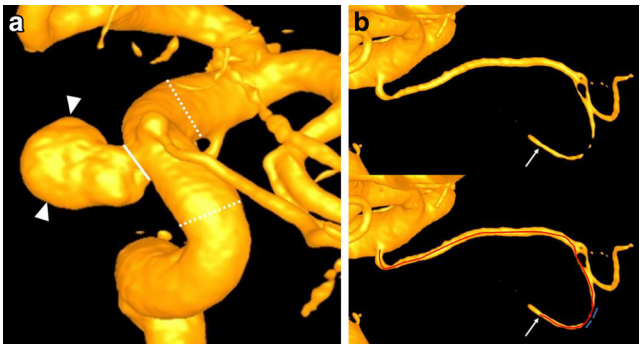

Fig. 3 An example of the results of quantitative evaluation is shown below. **a** The diameter of the aneurysm (*white arrowheads*), the neck diameter (*white line*), and the parent vessel diameters (each 5 mm from the neck end; *white dotted lines*) are measured at the WA (working angle). **b** At the angle where the AChA (anterior choroidal artery) appears longer, the length from the origin to a defined arbitrary point (*white arrow*) on the AChA (d1; *red line*) and the length that could not be visualized (d2; *blue line*) are measured

Statistical Analysis

Qualitative parameters (e.g., visualization of the aneurysm and AChA) were analyzed using paired t-test. The inter-rater reliability between the three reviewers was assessed using Fleiss's Kappa statistic. A Kappa index ≤ 0.40 was considered poor agreement, a Kappa index between 0.41 and 0.60 was considered moderate agreement, a Kappa index between 0.61 and 0.80 was considered good agreement, and a Kappa index between 0.81 and 1 was considered excellent agreement [11].

Quantitative parameters (e.g., diameters of the aneurysm and the AChA) were plotted on scatter plots, and regression analysis was performed. Intra-class correlation function was calculated using the formula presented in the study by Shrout et al. [12]. The evaluation index was the same as the Kappa index.

All statistical analyses were performed using Excel (version 2019; Microsoft, USA) and R4.0.2 (CRAN). Statistical significance was set at $p < 0.05$.

Results

Patient Characteristics

Twenty consecutive patients (seven men and thirteen women; mean age: 53.1 ± 12.7 years) with unruptured and untreated CA were included in this study. All the patients were successfully injected with contrast medium, and 3D-DSA and 3D-A reconstructions from the 3D-DSA micro datasets were successfully post-processed and evaluated.

Table 1 Patient characteristics

Number of cases	**20**
Age, years	53.1 ± 12.7
Female sex, number (%)	13 (65)
Aneurysm details	
Maximum diameter, cm	5.9 ± 1.4
Dome diameter, cm	4.9 ± 1.4
Neck diameter, cm	3.4 ± 1.3
Location	**Number (%)**
ACA	1 (5)
AcomA	6 (30)
MCA	1 (5)
ICA-AChA	2 (10)
ICA-PcomA	5 (25)
ICA-cavernous	5 (25)

Variables are expressed as mean ± standard deviation or as number (%)
ACA anterior cerebral artery; *AcomA* anterior communicating artery; *MCA* middle cerebral artery; *ICA* internal cerebral artery; *AChA* anterior choroidal artery; *PcomA* posterior communicating artery

Table 2 Evaluation of qualitative parameters

	3D-DSA micro	3D-A	P value
Aneurysm	3.7	3.6	0.07
AChA			
a	2.7	2.5	0.12
b	3.2	3.1	0.10
c	3.2	3.0	0.12
d	2.6	2.3	<0.05
e	1.8	1.2	<0.01

The visualization quality of 3D-DSA and 3D-A images of the aneurysm and each of the five points on AChA was evaluated. Each point on AChA was defined in Fig. 2 and shown in Fig. 4 as an example. The recorded scores were means of the scores awarded by the reviewers
3D-DSA three-dimensional digital subtraction angiography; *3D-A* three-dimensional angiography; *AChA* anterior choroidal artery

The patient characteristics, including aneurysm details, are summarized in Table 1.

Evaluation of Qualitative Parameters

Evaluation of visualization quality between 3D-DSA and 3D-A images was performed. In the aneurysm evaluation, 3D-DSA and 3D-A reconstructions showed comparable visualization qualities. In the AChA evaluation, both reconstructions showed similar visualization qualities at points a, b, and c. The visualization quality at points d and e was higher with 3D-DSA than with 3D-A. The summary of the analysis is shown in Table 2. A simple example is shown in Fig. 4.

The inter-observer agreements between the three reviewers for the aneurysm and the five points on the AChA were good (i.e., Kappa index ≥ 0.60).

Evaluation of Quantitative Parameters

The reviewers measured the degree of accuracy between 3D-DSA and 3D-A images. Quantitative assessment of the corresponding 3D-DSA and 3D-A images revealed identical results in terms of the aneurysm diameter at the designated location, the neck diameter, and the parent vessel diameter. The results are shown as distribution maps and regression analysis in Fig. 5a. The mean percentage of AChA length that could be visualized was significantly higher in 3D-DSA images than in 3D-A images (3D-DSA: 96.4%, 3D-A: 88.2%, P < 0.05). An example is shown in Fig. 5b.

The inter-observer agreements between the three reviewers for quantitative assessment were excellent in all cases.

Discussion

Currently, 3D-DSA is regarded as the standard in the diagnostic work-up of cerebrovascular disease. However, approximately 50% of the exposure dose required for 3D-DSA is needed to capture the mask, and the subtraction method is susceptible to artifacts caused by misalignment of the mask and fill runs [13]. Several previous studies have reported on the need to reduce the exposure dose and the artifacts during 3D-DSA (e.g., by lowering the dose per frame or 3D rotational angiography) [14–16]. However, these imaging techniques may have limitations in terms of reliability to reproduce blood vessels [17]. Due to problems regarding radiation dose and motion artifact, a technique to reduce radiation dose and obtain diagnostic information at the same time was highly desired. Therefore, the AI-based 3D-A technique was developed to obtain 3D-DSA-like im-

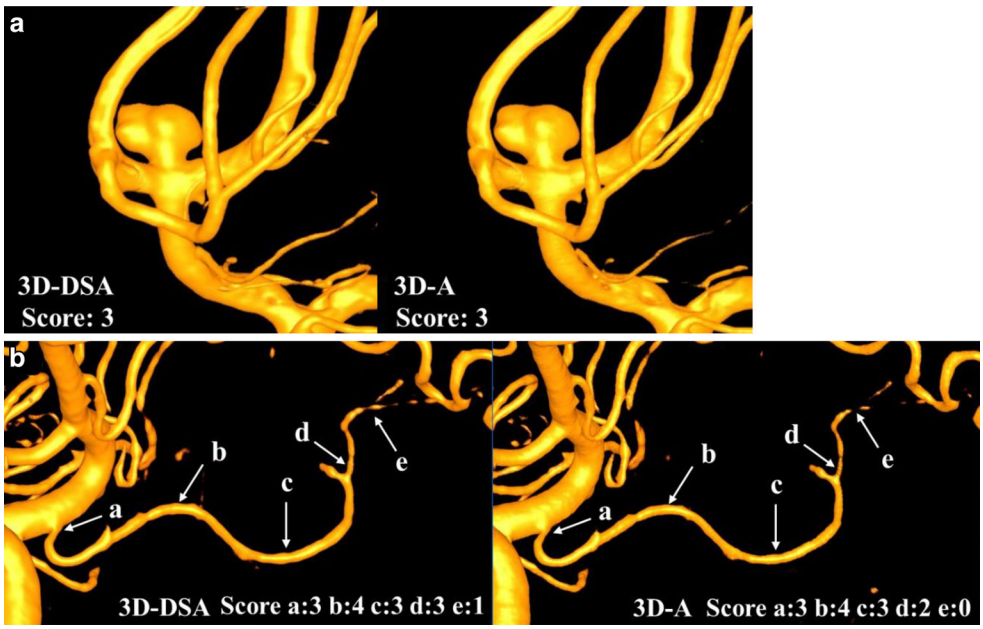

Fig. 4 An example of the results of qualitative evaluation is shown above. AcomA (anterior communicating artery) aneurysm in a 48-year-old man (case number 3). **a** 3D-DSA (three-dimensional digital subtraction angiography) and 3D-A (three-dimensional angiography) images of the aneurysm. **b** 3D-DSA and 3D-A images showing five points on the AChA (anterior choroidal artery). The 3D-DSA and 3D-A reconstructions are comparable in terms of visualization of the aneurysm and points a, b, and c on the AChA. However, visualization of points d and e is better with 3D-DSA than with 3D-A. The recorded scores are the means of the scores awarded by the reviewers

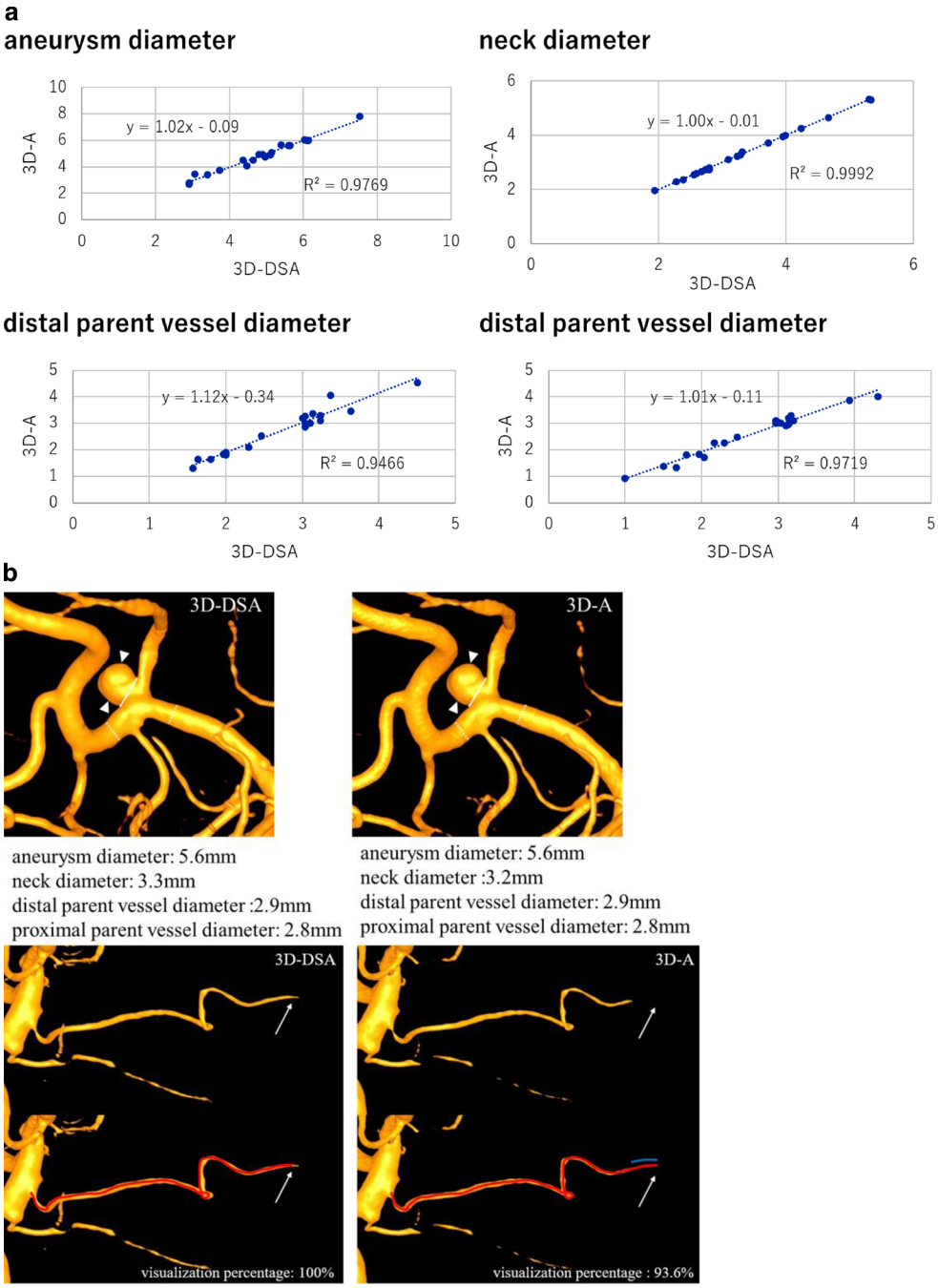

Fig. 5 The quantitative evaluation of one patient is shown above. **a** Distribution maps of the aneurysm diameter at a designated location, the neck diameter, and the parent vessel diameter (horizontal axis: 3D-DSA (three-dimensional digital subtraction angiography), vertical axis: 3D-A (three-dimensional angiography)) The statistics are based on the means of the scores awarded by the reviewers. The results of the regression analysis are almost the same. **b** AcomA (anterior communicating artery) aneurysm in a 53-year-old man (case number 6). The aneurysm diameter, neck diameter, and parent vessel diameter determined with 3D-DSA and 3D-A are almost equal. The percentage of AChA (anterior choroidal artery) length that could be visualized was higher with 3D-DSA than with 3D-A

ages during single contrast scans. With the AI-based algorithm already validated for normal vessels, CAs, dAVFs, and AVMs, the potential of the technology to generate diagnostic quality was reported in previous studies [7–9]. In the previous studies, only conventional 3D-DSA imaging was evaluated, but 3D-DSA micro imaging, which allows for more detailed vascular diagnosis, was not validated. The 3D-DSA micro technique uses 1 × 1 binning, instead of the usual 2 × 2 binning, and it adapts imaging parameters, such as small field-of-view, for visualization of small objects to obtain high image quality. Furthermore, by optimizing exposure parameters and image processing algorithms, 3D-DSA micro imaging can offer local spatial resolution higher than that of conventional 3D-DSA. Li et al. demonstrated the usefulness of high-resolution C-arm computed tomography (DynaCT Micro; Siemens) which is similar to 3D-DSA micro technique [18]. For these reasons, 3D-DSA micro imaging has been used to evaluate aneurysm shape, nearby vessel diameter, branching vessels, and perforating branches in the treatment of CAs. 3D-DSA micro imaging is more clinically important and more frequently used than 3D-DSA in actual clinical practice. Therefore, it is neces-

sary to evaluate AI-based 3D-A in 3D-DSA micro datasets using a similar algorithm before introducing 3D-DSA micro imaging to clinical practice. This study is the first study to demonstrate the efficacy of AI-based 3D-A for 3D-DSA micro imaging. Although we considered only CA in this study, by evaluating more clinical parameters and clarifying the evaluation criteria, we provided essential elements for the re-evaluation of the AI-based algorithm in preparation for their future implementation in clinical settings.

In our cases, the reconstructions of AI-based 3D-A were feasible in 3D-DSA micro images. In the clinical endovascular treatment of aneurysms, information on the size and neck of aneurysms is essential for appropriate coil selection, and the diameters of vessels distal and proximal to the aneurysm are also important to determine the stent size in stent-assisted coiling. Our result that the visualizations and diameters of the aneurysm and vessels around the aneurysm of AI-based 3D-A are equal to that of 3D-DSA, can be applicable to clinical endovascular treatment of aneurysms. Another important aspect in aneurysm treatment is to prevent occlusion of branching or perforating vessels. Based on our study results, visualization of proximal vessels with 3D-A is comparable to that with 3D-DSA. Hence, 3D-A also can be useful for recognizing the origins of bifurcating vessels.

A previous study reported the usefulness of 3D-A for the visualization and diagnosis of vascular malformations such as dAVF and AVM [9]. Considering the poor distal vessel delineation of 3D-A images observed in this study, we posited that 3D-A is not suitable for vascular malformations such as dAVF and AVM because adequate delineation of distal portions of vessels is essential in cases of vascular malformation. The poor distal vessel delineation may be due to the diameter of the vessels and not because the vascular imaging protocol (5-second 3D-DSA micro) used in this study is different from those used in previous studies. Vascular malformations with shunts (such as dAVF and AVM) are associated with high blood flow and large peripheral vessels that allow for adequate delivery of contrast medium. Good delineation may be achieved by increasing contrast volume, changing image protocols, and adjusting window levels and thresholds for adequate visualization. We did not evaluate vascular malformations in this study, but we would like to evaluate them in future studies.

Finally, all the patients in our study were treated with local anesthesia. Our study results showed the effectiveness of local anesthesia and are comparable to those of previous studies. In cases where patients are treated with local anesthesia, subtraction techniques that require two rotations are susceptible to motion artifacts due to misregistration of the mask and fill runs. AI-based 3D-A imaging with single rotational acquisition reduces the chance of motion from mechanical instability or patient motion [7–9]. We posit that this technique may be useful for some patients who have difficulty undergoing general anesthesia and can only be treated with local anesthesia. Moreover, the safety of flow diverter treatment for aneurysms under local anesthesia and the efficacy of angioplasty of intracranial vessels with neurological monitoring have recently been reported [19–21]. AI-based 3D-A can also be used in the above-mentioned cases in clinical practice.

Limitations

This study has some limitations. First, the number of patients in this study was relatively low, and comparison with cases of posterior circulation or aneurysm diameter ≥ 10 mm was not performed in this study. Second, our study only included patients without previous treatment for vascular lesions, and it did not address the eligibility of the prototype 3D-A technique for the visualization of metallic implants (e.g., coil, stent, and liquid embolic material). Third, the 3D-A threshold was evaluated at a constant value of 40%. Since adjusting the value changes the degree of visualization of perforating vessels and other vessels, it is possible that visualization of the distal AChA may have changed after setting an appropriate threshold, adjusting the amount of contrast agent used, or adjusting the window level. In this study, the threshold parameter was fixed improve comparability. To address the above-mentioned limitations, additional studies with more detailed conditions should be conducted. Furthermore, new protocols for contrast agent injection speed and volume and for imaging rotation speeds that account for metal artifacts should be devised and incorporated into the AI algorithm. The acquisition protocol used in this study was necessary to facilitate the clinical use of AI-based 3D-A, and there is still room for the improvement of the new technique.

Conclusions

The AI-based 3D-A technique is feasible and evaluable in 3D-DSA micro imaging. Regarding diagnostic potential, visualization of the angioarchitecture of the aneurysm and the diameters of vessels around the aneurysm with 3D-A is equal to that with conventional 3D-DSA. The 3D-A technique offers the same degree of visualization of the proximal portion of the AChA as 3D-DSA, but it offers lower visualization of the distal portion of the AChA than 3D-DSA. Further improvements and clinical applications of AI-based 3D-A in the future will require optimization of injection protocols and standardization of reconstruction.

Acknowledgements The authors would like to thank Philipp Roser and Iwao Kojima for lending their expertise on the Artificial Intelligence-Based 3D-Angiography. We also gratefully acknowledge Naoki Kato, Nobuhisa Fukaya, Kazuki Ishii for your participation and help in our study.

Funding This study was partly supported by Siemens Healthcare, K.K under a collaboration research agreement with Department of Neurosurgery, Nagoya University. The prototype software, 3D angiography was provided by Siemens Healthcare, K.K. Partial financial support was received from Siemens Healthcare, K.K.

Author Contribution All authors: Conceptualization; K. Ishikawa: Material preparation and data collection, Data analysis, Writing—original draft preparation; T. Imaizumi: Data analysis, Writing—review and editing; M. Nishihori: Writing—review and editing; R. Saito: Supervision; All authors have approved the submitted version of the manuscript and agreed to be accountable for any part of the work.

Declarations

Conflict of interest K. Ishikawa, T. Izumi, M. Nishihori, T. Imaizumi, S. Goto, K. Suzuki, K. Yokoyama, F. Kanamori, K. Uda, Y. Araki and R. Saito declarethat they have no competing interests.

Ethical standards All procedures performed in studies involving human participants or on human tissue were in accordance with the ethical standards of the institutional and/or national research committee and with the 1975 Helsinki declaration and its later amendments or comparable ethical standards. The study protocol was approved by the local intuitional review board of Nagoya University (2016-0194). Informed consent was obtained from all individual participants included in the study.

References

1. Wong SC, Nawawi O, Ramli N, Kadir AKA. Benefits of 3D rotational DSA compared with 2D DSA in the evaluation of intracranial aneurysm. Acad Radiol. 2012;19:701–7. https://doi.org/10.1016/j.acra.2012.02.012.
2. van Rooij WJ, Sprengers ME, de Gast AN, Peluso JP, Sluzewski M. 3D rotational angiography: the new gold standard in the detection of additional intracranial aneurysms. AJNR Am J Neuroradiol. 2008;29:976–9. https://doi.org/10.3174/ajnr.A0964.
3. Lauriola W, Nardella M, Strizzi V, Cali A, D'Angelo V, Florio F. 3D angiography in the evaluation of intracranial aneurysms before and after treatment. Initial experience. Radiol Med. 2005;109:98–107.
4. Anxionnat R, Bracard S, Ducrocq X, Trousset Y, Launay L, Kerrien E, et al. Intracranial aneurysms: clinical value of 3D digital subtraction angiography in the therapeutic decision and endovascular treatment. Radiology. 2001;218:799–808. https://doi.org/10.1148/radiology.218.3.r01mr09799.
5. Missler U, Hundt C, Wiesmann M, Mayer T, Brückmann H. Three-dimensional reconstructed rotational digital subtraction angiography in planning treatment of intracranial aneurysms. Eur Radiol. 2000;10:564–8. https://doi.org/10.1007/s003300050961.
6. Tanoue S, Kiyosue H, Kenai H, Nakamura T, Yamashita M, Mori H. Three-dimensional reconstructed images after rotational angiography in the evaluation of intracranial aneurysms: surgical correlation. Neurosurgery. 2000;47:866–71. https://doi.org/10.1097/00006123-200010000-00016.
7. Montoya JC, Li Y, Strother C, Chen GH. 3D deep learning angiography (3D-DLA) from C-arm conebeam CT. AJNR Am J Neuroradiol. 2018;39:916–22. https://doi.org/10.3174/ajnr.A5597.
8. Lang S, Hoelter P, Schmidt M, Eisenhut F, Kaethner C, Kowarschik M, et al. Evaluation of an artificial intelligence-based 3D-angiography for visualization of cerebral vasculature. Clin Neuroradiol. 2020;30:705–12. https://doi.org/10.1007/s00062-019-00836-7.
9. Lang S, Hoelter P, Schmidt M, Strother C, Kaethner C, Kowarschik M, et al. Artificial intelligence-based 3D angiography for visualization of complex cerebrovascular pathologies. Ajnr Am J Neuroradiol. 2021;42:1762–8. https://doi.org/10.3174/ajnr.A7252.
10. Goodfellow I, Bengio Y, Courville A. Deep learning. 1st ed. Cambridge: MIT Press; 2016.
11. Fleiss JL. Measuring nominal scale agreement among many raters. Psychol Bull. 1971;76:378–82. https://doi.org/10.1037/h0031619.
12. Shrout PE, Fleiss JL. Intraclass correlations: uses in assessing rater reliability. Psychol Bull. 1979;86:420–8. https://doi.org/10.1037/0033-2909.86.2.420.
13. Kim DJ, Park MK, Jung DE, Kang JH, Kim BM. Radiation dose reduction without compromise to image quality by alterations of filtration and focal spot size in cerebral angiography. Korean J Radiol. 2017;18:722–8. https://doi.org/10.3348/kjr.2017.18.4.722.
14. Pearl MS, Torok CM, Messina SA, Radvany M, Rao SN, Ehtiati T, et al. Reducing radiation dose while maintaining diagnostic image quality of cerebral three-dimensional digital subtraction angiography: an in vivo study in swine. J Neurointerv Surg. 2014;6:672–6. https://doi.org/10.1136/neurintsurg-2013-010914.
15. Pearl MS, Torok C, Katz Z, Messina SA, Blasco J, Tamargo RJ, et al. Diagnostic quality and accuracy of low dose 3D-DSA protocols in the evaluation of intracranial aneurysms. J Neurointerv Surg. 2015;7:386–90. https://doi.org/10.1136/neurintsurg-2014-011137.
16. Raabe A, Beck J, Rohde S, Berkefeld J, Seifert V. Three-dimensional rotational angiography guidance for aneurysm surgery. J Neurosurg. 2006;105:406–11. https://doi.org/10.3171/jns.2006.105.3.406.
17. Hirai T, Korogi Y, Suginohara K, Ono K, Nishi T, Uemura S, et al. Clinical usefulness of unsubtracted 3D digital angiography compared with rotational digital angiography in the pretreatment evaluation of intracranial aneurysms. Ajnr Am J Neuroradiol. 2003;24:1067–74.
18. Li TF, Ma J, Han XW, Fu PJ, Niu RN, Luo WZ, et al. Application of high-resolution C-arm CT combined with streak metal artifact removal technology for the stent-assisted embolization of intracranial aneurysms. Ajnr Am J Neuroradiol. 2019;40:1752–8. https://doi.org/10.3174/ajnr.A6190.
19. Griessenauer CJ, Shallwani H, Adeeb N, Gupta R, Rangel-Castilla L, Siddiqui AH, et al. Conscious sedation versus general anesthesia for the treatment of cerebral aneurysms with flow diversion: a matched cohort study. World Neurosurg. 2017;102:1–5. https://doi.org/10.1016/j.wneu.2017.02.111.
20. Rajbhandari S, Matsukawa H, Uchida K, Shirakawa M, Yoshimura S. Clinical results of flow diverter treatments for cerebral aneurysms under local anesthesia. Brain Sci. 2022;12:1076. https://doi.org/10.3390/brainsci12081076.
21. Chamczuk AJ, Ogilvy CS, Snyder KV, Ohta H, Siddiqui AH, Hopkins LN, et al. Elective stenting for intracranial stenosis under conscious sedation. Neurosurgery. 2010;67:1189–93. https://doi.org/10.1227/NEU.0b013e3181efbcac. discussion 1194.